Excitonic states and structural stability in two-dimensional hybrid organic-inorganic perovskites

Lekina, Yulia; Shen, Ze Xiang

2019

Lekina, Y., & Shen, Z. X. (2019). Excitonic states and structural stability in two-dimensional hybrid organic-inorganic perovskites. Journal of Science: Advanced Materials and Devices, 4(2), 189-200. doi:10.1016/j.jsamd.2019.03.005

https://hdl.handle.net/10356/141930

https://doi.org/10.1016/j.jsamd.2019.03.005

Journal of Science: Advanced Materials and Devices 4 (2019) 189–200

Contents lists available at ScienceDirect

Journal of Science: Advanced Materials and Devices

journal homepage: www.elsevier.com/locate/jsamd

Review Article

Excitonic states and structural stability in two-dimensional hybrid organic-inorganic perovskites

Yulia Lekina, Ze Xiang Shen*

Division of Physics and Applied Physics, School of Physical and Mathematical Sciences, Nanyang Technological University, SPMS-04-01, 21 Nanyang Link, 637371, Singapore

ARTICLE INFO

Article history:
Received 26 March 2019
Accepted 27 March 2019
Available online 3 April 2019

Keywords:
Two-dimensional perovskites
Layered perovskites
Excitons
Excitonic states
High pressure
Photoluminescence
Solar cells
Light emitting diodes

ABSTRACT

Two-dimensional (2D) perovskites are a new class of functional materials that may find applications in various technologically important areas. Due to the better moisture and illumination stability, layered perovskites can be the next generation of materials for solar light-harvesting applications, as well as for light emitting diodes (LEDs). Besides, extended chemical engineering possibilities allow obtaining advanced perovskite materials with desirable functional properties, such as tunable band gap, strong exciton-phonon coupling, white light emission, spin-related effects, etc. A full understanding of the fundamental properties is essential for developing new 2D perovskite-based technologies. In this paper, recent reports on 2D perovskites are reviewed, including the synthesis methods of single crystals, nanosheets and films; the crystal and electronic structures; the excitonic states and interactions; the properties of the materials under low temperature and high pressure; and a brief discussion on the challenges in understanding the fundamental properties of the layered perovskites.

1. Introduction

Since the first mineral with the perovskite structure $CaTiO_3$ was discovered in 1839 [1], various materials repeating this crystal motif, perovskite-like materials, have been discovered. These compounds have demonstrated various functional properties such as ferroelectricity [1], nonlinearity [2], semiconductivity [3], colossal magnetoresistance [4], multiferroic features [5].

Traditionally inorganic materials (mostly oxides) are known to have perovskite-like structure, but recently hybrid organic-inorganic and all inorganic [3] halides have attracted intense attention due to their high performance and low cost in solar cells applications [3,6,7]. Moreover, this class of materials has been shown to be promising to use in light emitting diodes [6,8,9], X-ray-, photodetectors [10,11], spintronics [12], batteries [13], and lasing [14]. Development of the solar cell performance of hybrid halide perovskites with the general formula AMX_3 (A is an organic cation, usually MA = CH_3-NH_3^+ or FA = NH_2-CH-NH_2^+; M = Pb, Sn; X = I, Br, Cl or a mixture of them) is much faster than that of other photovoltaic materials [6,15]. Moreover, altering the composition allows tuning the band gap and optical properties of the material efficiently [15].

However, poor moisture and illumination stability of regular three-dimensional (3D) hybrid organic-inorganic perovskites still remains the main obstacle to fabricate the low-cost and long-running devices [6,12]. Two-dimensional (2D) perovskites, demonstrating better stability and extended chemical engineering possibilities, can be the next generation of materials for solar light-harvesting applications [16], as well as for light emitting diodes (LEDs) [12,17–22].

2D perovskites represent a particular class of low-dimensional perovskites, that can be obtained from the parent perovskite structure by slicing it along one of the crystallographic planes and inserting a long organic cation between, yielding a layered structure with corner-sharing octahedral inorganic quantum wells separated by an organic barrier. In practice, it is achieved by substitution of a small cation at the A position of AMX_3 by a bulk amine R^+. In case if only a part of A is substituted, so-called multilayered perovskites can be obtained [23,24]. The generic chemical formula of the multilayered perovskites with corner-sharing octahedra is $R_2(A)_{n-1}M_nX_{3n+1}$ (if R is a monobasic amine), where n represents the number of octahedral layers within one inorganic sheet (Fig. 1) [25]. Higher members of R_2 $(MA)_{n-1}Pb_nI_{3n+1}$ ($n > 2$) have attracted a lot of

* Corresponding author.
E-mail addresses: yulia001@e.ntu.edu.sg (Y. Lekina), zexiang@ntu.edu.sg (Z.X. Shen).

Peer review under responsibility of Vietnam National University, Hanoi.

https://doi.org/10.1016/j.jsamd.2019.03.005

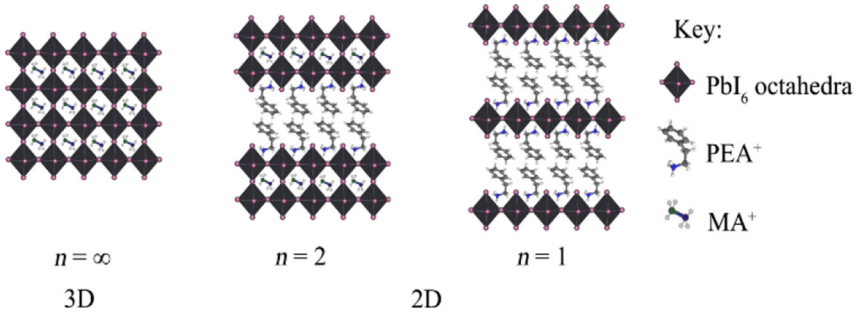

Fig. 1. Schematic representation of multilayered perovskites on the example of $PEA_2(MA)_{n-1}PbnI_{3n+1}$.

attention recently due to high efficiency at solar cell application [17,26–29]. Improved stability of the perovskites with $n = 10, 40, 60$ was emphasized, while power conversion efficiency (PCE) was shown to reach 15.6% [26]. The $n = 4$ member demonstrated the efficiency up to 13% [28,30] while the heterostructured 3D-2D perovskites exhibit PCEs up to 17–19% [31]. Such materials have been found to be perfect materials for light-emitting diodes (LEDs) due to tenability, high quantum efficiencies, and broadband emission [12,17–21,31].

Besides, 2D perovskites exhibit special properties in comparison with their 3D analogous. Their natural quantum-well structure yields stable excitons, able to interact more strongly with phonons, spins, and defects. Layered perovskites have been shown to be more structurally stable under non-ambient conditions than the 3D ones, with maintaining the same phase longer under increasing pressure or decreasing temperature [32–34]. In case of the existence temperature-caused phase transitions they are usually associated with the organic ions [32]. The unique properties make 2D perovskites good candidates for new advanced materials for various applications [35].

In this paper, we summarize the publications on the structural, electronic, and optical properties of 2-dimensional hybrid halide perovskites under ambient condition, high pressure, and various temperatures. The review is organized in the following way: first, structural features of 2D perovskites are discussed, followed by a brief overview of the synthetic approaches for both crystals and films. Second, the electronic and optical properties of various compounds are presented. Then the excitonic effects, such as coupling and trapping, are reviewed in details. Finally, we analyze the structural stability of 2D perovskites and the phenomena caused by applying non ambient conditions. Various applications of the layered perovskites are beyond the scope of this work, they have been reviewed in details before (refer to [36–38]).

2. Crystal structure, motifs and orientation in films.

In case of regular 3-dimensional perovskites, the sizes of the *A*, *B* and *X* ions are to fit the certain ratio to form perovskite-like structures. The ability to form a perovskite-like structure is determined by the Goldschmidt tolerance factor *t* [39,40]:

$$t = \frac{R_A + R_X}{\sqrt{2}(R_B + R_X)} \quad (1)$$

For perovskite-like 3D crystal structures, the Goldschmidt Tolerance Factor usually is $0.8 < t < 1$ [39], that strictly limits the radius of the cation *A*.

For two-dimensional perovskites $R_2(A)_{n-1}M_nX_{3n+1}$, the same rule applies to the *A* cations. The rule is relaxed for the organic cation *R*, and *R* can take various values. *R* still needs to obey a few restrictions. Firstly, *R* must contain at least one terminal cation group, which can form hydrogen bonds with the inorganic anions. Usually, one or two protonated terminated amines take part in forming hybrid layered structures. Secondly, the size and shape of the organic molecule *R* influence the formation of the layered structures. The molecular cross-section (the projection down the long axis of *R*) must be approximately equal to the area between terminal halides of the inorganic framework. In case of lead iodide, this is a square of ~40 $Å^2$. However, the length of the organic cation *R* can take on a wide range of values. In fact, it just needs to be longer than the size of the vacancy between inorganic octahedra [25] to prevent the formation of 3D perovskites.

Moreover, interactions between the *R* cations can stabilize or destabilize the structure due to Van der Waals, aromatic–aromatic π-interactions [25], and hydrophobic forces [41]. It should be also noted that in contrast with disordered MA in cubic 3D structures [24], longer cations in 2D perovskites are in fact rigid due to van der Waals forces and in some cases π-π interactions [42].

The nature of *R* cation has been shown to significantly affect the structure of 2D perovskites [25,42]. The layered hybrid perovskites with $R = PhC_mH_{2m}NH_3$ illustrate this phenomenon (Fig. 2). Despite these cations apply to the same homologous series, the length of the alkyl part affects not only lattice parameters but also stoichiometry and ordering of the inorganic octahedra, including the direction of the planes and type of sharing. And this is not the only example of different types of octahedral ordering. In general, the case where the octahedral layers are flat and located along <001> plane is the most common type [25,43]. Alkylammonium metal halides are the most common examples, in which the compounds with the general formula $C_xH_{2x+1}MX_4$ (where $x = 4–10$, M = Pb, Sn, Ge, X = Cl, Br, I) [33,44–47] have been reported to exhibit the <001> arrangement of octahedra as well as their solid solutions with various concentrations of Cl/Br/I components [48,49]. Another group of compounds, known to be of this type, are phenylethyl ammonium metal halides [50,51]. Histammonium and benzylammonium lead and tin iodides has been reported to follow the <001> structure type as well [52].

The <110>-type of layered perovskites is less common. Compounds containing the iodoformamidinium cation are of this type [25,43,53] as well as compounds with two ammonium groups in the organic cation. For example, α-(DMEN)$PbBr_4$ (2-(dimethylamine)ethylamine) is known to be a "3 × 3" <110> perovskite. Local hydrogen bonding of the "chelating" effect causes the unique bending of the inorganic layers [54]. In this case, the corner shared octahedra layers form folds, and 3 × 3 means that the width of the folds is equal to 3 octahedra. However, many of the perovskites with two amino groups do not follow this rule, for instance, (EDBE)$PbCl_4$, $H_3N(CH_2)_6NH_3PbBr_4$, and (AEQT)$PbBr_4$ (AEQT = 5,5‴-bis(aminoethyl)-2,2′:5′,2″:5″,2‴-quaterthiophene) are <100> while (EDBE)$PbBr_4$ is <110> (EDBE = 2,2-(ethylenedioxy)bis-

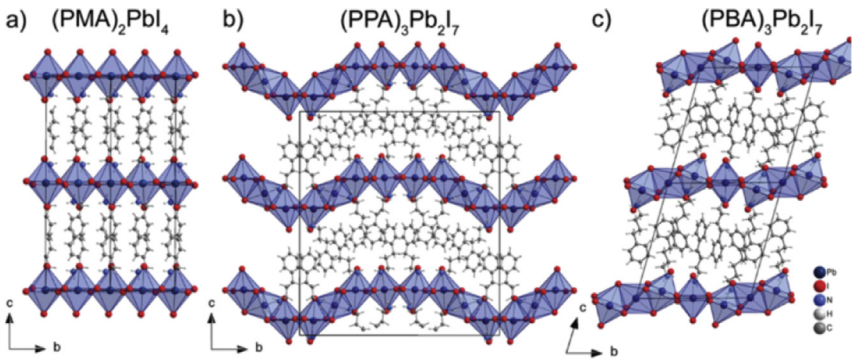

Fig. 2. Structural motifs of the RPb_xI_y layered perovskites. a) Structure of $PhCH_2NH_3$-PbI and $PhC_2H_4NH_3$-PbI. b) Structure of $PhC_3H_6NH_3$-PbI. c) Structure of $PhC_3H_6NH_3$-PbI. b) and c) Structures contain both face-sharing and corner-sharing octahedra; a) Structures contain only corner-sharing octahedra [42]. Reprinted with permission from [42]. Copyright (2016) American Chemical Society.

(ethylammonium)) [55–58]. The compounds, containing cyclohexylammonium cation, are known to form <111>-oriented 2D perovskites. Moreover, there are some exotic types of layering [43].

One more class of 2D perovskites is worth to discuss. So-called "multilayered" or quasi-2D perovskites can be obtained from 3D compounds by substitution of the part of small A^+ cations with a longer R^+ one [23,24]. Thus, these materials contain both A^+ and R^+ cations. The generic chemical formula of the multilayered perovskites is $R_2(MA)_{n-1}Pb_nX_{3n+1}$, where R is a monobasic amine; X is halide; and n represents a number of octahedral layers within one inorganic sheet (Fig. 1). The most common 2D perovskites contain methylammonium (MA), lead (Pb), but the tin-based [59] and formamidinium-based [60] multidimensional perovskite have been described as well.

Depending on the type of the organic cations and relative stacking of the inorganic layers, all <100> oriented layered hybrid organic-inorganic perovskites can be divided into four categories: Dion-Jacobson – DJ (Fig. 3a) [61,62], Ruddlesden-Popper – RP (Fig. 3b) [41], perovskites with alternating cations in the interlayer space – ACI (Fig. 3c) [63], and Aurivilius - AV [63] (known only among oxide perovskites) phases. RP perovskites contain a pair of monobasic ammonium (R^+) and offset stacking of the inorganic layers along both a and b directions [41]. DJ perovskites, containing one interlayer dibasic ammonium cation (R^{+2}), can form layers arranged one strictly above the other [62], or shifted by a half of the octahedron along only a or b direction [61]. The phase with alternating cations in the interlayer space is similar to DJ perovskites in terms of the displacement of the inorganic layers only along one of a or b directions. However, this class contains two types of the organic cations in the interlayer space. ACI perovskites were reported to exhibit decreased band gap in comparison with the PR analogous [63].

Out-of-plane charge transport in layered perovskites is significantly obstructed, therefore the orientation of thin films plays a critical role in the application of 2D perovskites. The compounds with small values of n demonstrate a high degree of inorganic octahedral sheets parallel to the substrate surface [64]. For instance, in the methyl-butylammonium perovskite series only the $n = 1$ member tends to grow with its inorganic planes parallel to the substrate surface, while $n = 2$ grown with the octahedral planes parallel to the substrate as well as along other directions. The perovskites with $n \geq 3$ tend to grow vertical layers [23,65], and this has been explained by the preferential growth at the liquid–air interface of the precursor solution, regardless the roughness or material of the substrate [66].

Vertically grown inorganic layers were shown to dramatically improve solar cell performance of the Ruddlesden-Popper phase perovskite thin films [66]. A few methods to improve crystallinity and degree of the vertical orientation were proposed. First, adding NH_4SCN and NH_4Cl to the precursor solution was shown to tune the orientation and to decrease a concentration of nonradiative defects yielding 14.1% PCE for the $n = 5$ methyl-phenylethyl-ammonium perovskite [67]. The second way to improve orientation and crystallinity is to produce films by hot-casting instead of conventional spin-coating [28]. Varying solvents may help as well, for instance, better films of the hot-casted $n = 5$ butyl-based perovskite were obtained from 3:1 DMF:DMSO solution than from the pure DMF or DMSO alone. Nature of the organic cation was shown to affect the

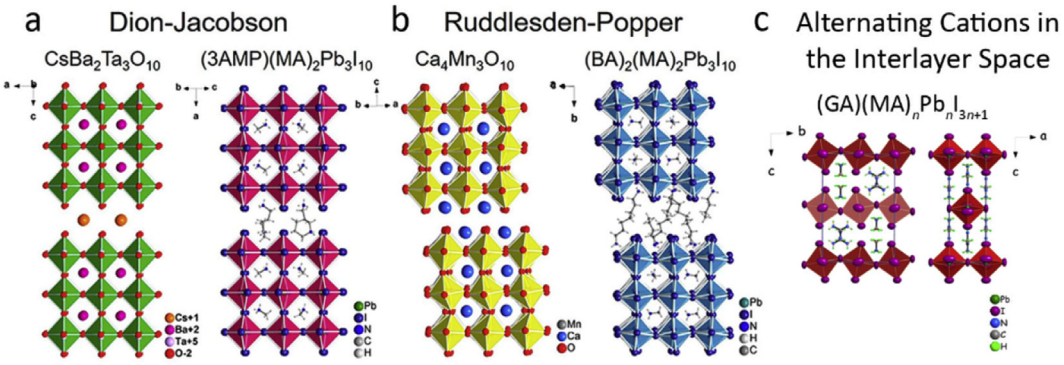

Fig. 3. Examples of Dion-Jacobson DJ (a), Ruddlesden-Popper RP (b), and alternating cations in the interlayer space (ACI) (c) 2D perovskite phases. Adapted with permission from reference [62] (a, b) and [63] (c). Copyright (2017, 2018) American Chemical Society.

orientation as well, for instance substitution of *n*-buthylammonium with *iso*-buthylammonium produces $n = 4$ perovskites with better vertical orientation of the films [68]. In contrast with the mentioned above $n = 3$ RP perovskites, as well as the DJ perovskites [62], the $n = 3$ ACI perovskite grows in preferred horizontal orientation [63].Crystal structure, motifs and orientation in films.

3. Synthesis

Here we provide a brief overview of the most frequently used approaches to synthesize 2D perovskites.

One of the oldest methods is the silica gel technique, used by Ishihara in the first works on alkylammonium 2D perovskites. The idea of the method is diffusion of cations through the gel for a very slow rate of crystal growth [69,70]. However, the crystals obtained by the gel method are easily contaminated and it is quite difficult to control the gel hardness [32]. Another way to obtain the crystals (more appropriate for a shorter chain: butyl or hexyl ammonium) is slow evaporation of an aqueous solution of the precursors [70]. Ishihara also proposed to use a mixture of acetone and nitromethane as a solvent for the reaction. This method allowed to obtain a higher member perovskite ($n = 2$ phenyl ethyl ammonium lead iodide) as well [71].

Nowadays the aqueous solution crystallization method is normally applied to obtain crystalline samples of the Ruddlesden-Popper series. Stoichiometric amounts of PbO (or PbI_2), *R*I, MAI are dissolved in a mixture of aqueous HI and aqueous H_3PO_2 during boiling. Slow cooling to room temperature yields uncontaminated single crystals of the 2D perovskites - iodides [17,72–74]. Dion-Jacobson [62] and alternative cation perovskite [63] phases were obtained by similar HI solution method. This method is suitable for the rarer <111> oriented perovskites [75], Bromide perovskites [76] were crystallised from aqueous HBr solution using a similar approach (no H_3PO_2 is necessary). Alkyl ammonium lead bromides can be obtained by another solution method as well: antisolvent acetone is to be added to DMF solution of precursor [77].

The aqueous solution method was used for the preparation of tin-based perovskites. Since Sn^{+2} tends to be oxidised to Sn^{+4}, the oxygen-free atmosphere is recommended, although Cao et al. reported that the presence of H_3PO_2 is enough to prevent oxidation [78].

Spin-coating is an extremely important process for cheap and easily prepared devices, and good quality 2D perovskites films can be formed. Precursors [26,68,79,80] or solution of the final bulk material [77] in DMF or DMSO is usually used for spin coating, followed by annealing at 100 °C. Some authors recommend to carry out spin coating in a glove box with oxygen and moisture levels <0.1 ppm [68]. For tin-based perovskites, DMF and DMSO solutions of bulk material were used for spincoating [78]. MACl can be added to the precursor solution to improve the morphology of the films which have been used for perovskite solar cells [81].

For fundamental studies of the materials, high-quality thin crystals are often needed (Fig. 4). Mechanical exfoliation, similar to that used in exfoliating graphene, is the easiest way to obtain thin (up to a monolayer) crystals due to week interlayer bonding of the 2D perovskites [82–84]. Chemical Vapor Deposition (CVD) method is known to yield high-quality nano-crystals as well as films. 2D perovskites can be obtained by this method where the source of heavy PbX2 is placed closer to the deposition zone than the light organic halide [85]. Another method to obtain nano-size platelets is dropping a very dilute DMF-chlorobenzene precursor solution on the substrate followed by mild drying [44]. Besides, nano-plates were proposed to be converted from spin coated film by vapour annealing [86].

4. Stability

The main advantage of 2D perovskites over their 3D counterparts is the stability of thin films under illumination at ambient conditions. Encapsulated 2D perovskite-based solar cells retained 60% of their efficiency after an aggressive test: illumination of 100 mW/cm^2 for a duration of 2250 h; and they were also shown to be much more moisture stable than the 3D perovskites. Higher members of quasi-2D perovskite family were shown to be good candidates for photovoltaic applications due to their stability as well [87].

Even the addition of a small amount of 2D perovskites may yield an outstanding increase in the long-term stability of the all-inorganic 3D perovskite. Moreover, $CsPbI_3 \times 0.025$ $EDAPbI_4$ (EDA = ethylenediamine) perovskite thin film showed a PCE of 11.8%, that was a record for all inorganic perovskite solar cells, due to effective electron transfer and passivates the surface defects [88]. Presence of butylphosphonic acid 4-ammonium chloride was demonstrated to increase both the solar cell PCE and stability of $MAPbI_3$-based devices as well [89].

Treatment of the 3D perovskite surface with 2D perovskite was shown to be a good approach for more stable devices. 2D/3D interface $HOOC(CH_2)_4NH_3)_2PbI_4/MAPbI_3$ demonstrated ultra-stability and good performance [90]. Addition of butyl ammonium to the surface of FA/Cs-based collar cell gave a similar outstanding improvement of stability [31].

5. Electronic structure

Low dimensional perovskites exhibit the special properties due to their unique structure. The HOMO–LUMO energy gap of the organic molecules is usually much higher than the band gap of the inorganic layer [58]. Thus, natural multiple quantum-well

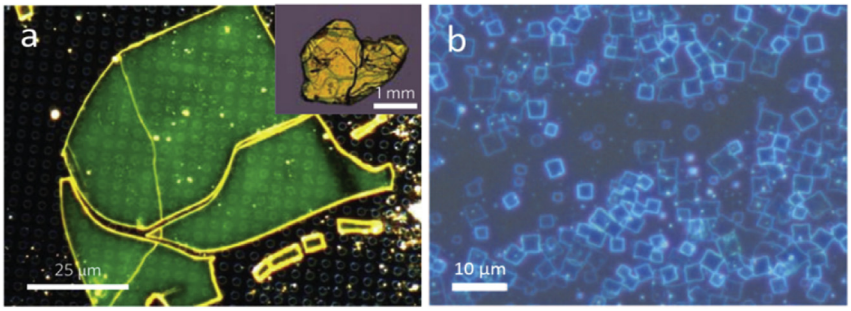

Figure 4. 2D perovskite thin platelets, obtained by a) mechanical exfoliation of a single crystal (adapted with permission from reference [82]. Copyright (2016) Springer Nature) and b) by dropping a very dilute DMF-chlorobenzene precursor. Adapted with permission from reference [44]. Copyright (2015) The American Association for the Advancement of Science.

structures are formed and the quantum confinement effect takes place due to low dimensionality of the semiconductor layers (potential walls), confined between optically inactive organic spacers (barriers) [41,42,91,92]. Quantum confinement depends on the thickness of the quantum well and of the barrier, for example, dimensionality, particularly the value of n in R_2 $(MA)_{n-1}Pb_nX_{3n+1}$ has been reported to dramatically affect its bandgap. Thus, the band gap and excitonic binding energy decrease with the parameter n increases [23].

Dielectric confinement should be considered along with the quantum confinement: the large difference between the dielectric constants of the organic barrier and the semiconducting layer is the additional enhancer and stabilizer of the excitons due to an image-potential-magnified attraction of charged particles (image charge effect) [93–95].

The quantum and dielectric confinement result in two main consequences. The first is the increased bandgap (and change of the form of the density of states) [96]. For instance, the band gap of the three dimensional $MAPbI_3$ is 1.51–1.61 eV [6,23,42], while the bandgap of the layered $(PEA)_2PbI_4$ is 2.22–2.24 eV [23,42]. The second consequence is the generation of stable excitons. Excitons are generally classified into two main classes: Frenkel or small excitons and Wannier or large excitons. The radius of small excitons is smaller than the unit cell parameters, that of Wannier excitons is larger. 3D hybrid perovskites were shown to form large excitons with binding energy E_b of 4–50 meV and radius of 2.2–3.8 nm. Small excitons with E_b = 500–1000 meV were found in various organic materials [43,96]. 2D perovskites exhibit strong excitonic absorption and luminescence even at room temperature. Excitonic binging energy was found to be 320 meV for $(C_{10}H_{21}NH_3)_2PbI_4$ (and was shown to increase with the length increasing) [32], 220 meV for PEA_2PbI_4 and 170 meV for $PEA_2MAPb_2I_7$ [94]. However, it is not possible to classify the excitons in 2D perovskite-based on the above simple classification. Some phenomena can be better explained by the model for Frenkel excitons, while the actual radii of the excitons are comparable to the unit cell size. In practice, this yields a strong sharp exciton luminescence and absorption even at room temperature [41,69,91] with short lifetimes (tens of picoseconds) [74,97].

Besides, improved enhancement of optical nonlinearity has been shown in butyl-methyl ammonium Ruddlesden-Popper series in comparison with the analogous. The 2D perovskites exhibited four times increase of third harmonic generation due to quantum confinement [98].

In general, theoretical models for first-principle calculations relevant to 2D hybrid organic-inorganic perovskites are much less developed that that of the 3D ones, and they require significant computational resources due to a very large number of atoms per unit cell. A detailed review of theoretical models for 2D perovskites is presented by Laurent Pedesseau et al. [12] and is beyond this work. Models based on an ultrathin quantum well with finite confinement barriers are shown to be applicable, detailed theoretical discussion of quantum confinement in 2D perovskites is published in reference 94 [99].

The electronic structures of 2D perovskites have been repeatedly shown to be mainly dependent on the inorganic sublattice, while organic cations demonstrate only indirect influence, such as steric effects [25,42,100]. The top of the valence band has been reported to be determined by Pb 6*s* and I 5*p* orbitals and the bottom of the conduction band by Pb 6*p* and I 5*s* ones [100]. However, the nature of organic cations has been found to significantly affect the crystal structure, including the crystal symmetry, bond length, and bond angle, distortion of octahedra, and even the type of octahedra arrangement [42,55,101]. These parameters have been shown to be tightly correlated with the electronic structure and optical properties. Bond contraction causes a decrease of bandgap due to greater orbital overlap [102]. Octahedral rotation induces weaker overlap and hence blueshift of bandgap [42,102]. Compounds with distorted octahedra have been shown to exhibit a broader emission, that is explained by the formation of trapped excitons due to higher defect concentration [42,54,101] or by self-trapping of excitons [55]. The type of octahedral ordering affects electronic structures as well, thus compounds with face-shared octahedra have been shown to exhibit blue shifted bandgap, compared with the corner-shared one, due to additional quantum confinement [103].

The above described quantum well model, that is hardly dependent on the organic cations, is true for most of 2D perovskites due to the large HOMO–LUMO gap of the organic cations. However, some compounds containing special functional organic molecules are exceptional cases. For example, introducing dye molecules into the structure as inorganic counter ion have been reported; 2D 5,5‴-bis-(aminoethyl)-2,2′:5′,2″:5″,2‴-quaterthiophene lead chloride exhibits emission was determined by the organic layer [104]. A similar effect was shown for naphthalene -based 2D perovskite, where efficient energy transfer from the inorganic to organic layer was observed, followed by naphthalene phosphorescence [105]. Introduction of some other opto-electronically active cations led to the formation of 1D or 0D perovskites, while electronic coupling between the organic ions and the inorganic lattice was kept strong [106,107].

Sudeep Maheshwari et al. introduced electron donating and electron withdrawing organic cations, resulting in the optical band gap determined by both the inorganic PbI_4 and organic molecule [108]. The band gap of electron donating 2,7-dibutylammonium [1] benzothieno [3,2-b]- [1]benzothiophene (BTBT) turned out lower (1.66 eV) than that of the other 2D perovskites. Introduction of the electron withdrawing groups, such as *N,N*-bis(*n*-butylammonium)-perylene-3,4,9,10-tetracarboxylic diimide (PDI), led to the much lower band gap of 0.11 eV. These results were obtained by calculations [108].

The organic layer may also affect the dielectric comfinement that can be decreased by introducing highly polarizable molecules. For instance, incorporating iodine molecules was shown to affect the electronic structure and optical properties of 2D perovskites significantly through decreasing the dielectric effect, resulting in a decrease in exciton binding energy to 50 meV [95]. Similar results were obtained by introducing highly polarised organic molecule, containing hydroxy group, as organic layer, e.g., the exciton binding energy of $(HOCH_2CH_2NH_3)_2PbI_4$ was found as low as that of 3D perovskite (13 meV) [109]. Reduced interlayer distance (2 Å) by using a short propane-1,3-diammonium bication allows to minimise quantum confinement as well, significantly enhancing interlayer charge transfer [30].

The fact that no interlayer electronic coupling was shown for conventional 2D perovskites (for example, alkyl ammonium or phenylethylammonium lead halides) and the quantum well structure implies that the band structure does not depend on number of layers, i.e. the optical properties of bulk 2D perovskite should not differ from that of a single layer sample. However, a shift of the optical properties has been demonstrated for atomically thin $(C_4H_9NH_3)_2PbBr_4$ sheet (single or double layer) in comparison with the bulk crystal. The difference resides in an unusual structural relaxation leading to a blue shift of the band gap of the single layer sample by ~5 nm [44].

6. Exciton–phonon interactions – excitonic states in 2D perovskites

Optical properties of 2D perovskites are dedicated by excitons, and that is why the investigation of intrinsic and extrinsic, radiative

and nonradiative exciton recombination pathways is essential. The intrinsic pathways are related to exciton-phonon interactions. Lattice vibrations create spatial and temporal potential fluctuations, where the first one causes scattering of excitons and broadening of excitonic peaks in optical spectroscopy, while the second leads to the fine structure of the spectra, known as Frank-Condon shape. Besides, a moving exciton is able to create vibrations around it, inducing lattice distortions [110](p. 203).

A few theories are used to describe the electron-phonon coupling. A model for the long wavelength acoustic phonons (LA) is called "Deformation Potential", and it gives the best approximation for the short-range interactions of charges with local changes in the crystal potential caused by the vibrations. Electrons interact with the optical phonons (only LO) as well, due to the microscopic electric field fluctuations in polar crystals. The second mechanism is called "Fröhlich interactions" and implies a long-range force. Piezoelectric interaction and interaction with nonpolar optical modes are known as well but are not important for 2D perovskites [110].

Exciton (electron) - phonon coupling is one of the reasons for emission spectra broadening. Dependence of full weight at half maximum (FWHM or Γ) of a PL peak on temperature allows extracting the coupling parameters and can be expressed as the following equation [111,112]:

$$\Gamma(T) = \Gamma_0 + \Gamma_{ac} + \Gamma_{LO} + \Gamma_{imp} = \Gamma_0 + \gamma_{ac}T + \gamma_{LO}\Big/\left(e^{h\omega_{LO}/k_BT} - 1\right) + \gamma_{imp}e^{-\frac{E_b}{k_BT}} \quad (2)$$

where Γ_0 represents FWHM at 0 K, which differs from zero due to the not infinite lifetime and inhomogeneous broadening caused by the disorder conditions and imperfections. Γ_{ac} and Γ_{LO} (homogenous) are caused by the exciton-phonon coupling with the acoustic and longitudinal optical phonon (of energy $h\omega_{LO}$, respectively; and the last term Γ_{imp} takes into account the exciton scattering (inhomogeneous) on ionized impurities with an average binding energy E_b. k_B is Boltzmann constant, γ represents exciton-phonon coupling strengths [111,112].

The terms Γ_{ac}, Γ_{LO} and Γ_{imp} give opposite contributions to the FWHM vs temperature plot (Fig. 5). Thus, the shape of the graph indicates which coupling is stronger, and fitting the experimental data allows to extract the coupling strength constants.

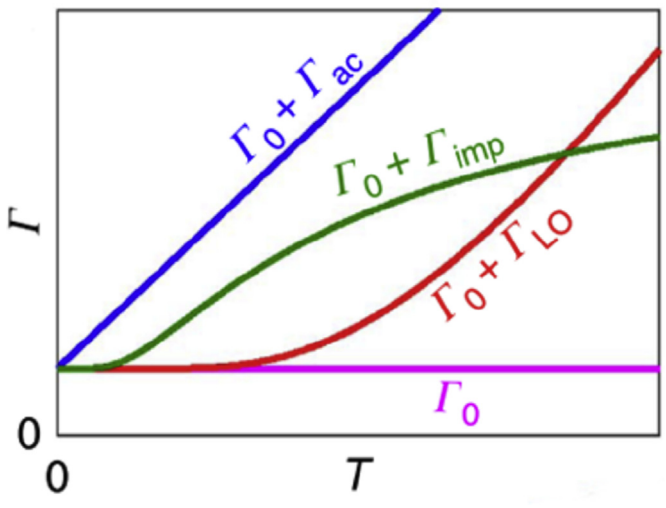

Fig. 5. Functional form of the dependence FWHM on temperature in case of different contributions. Reprinted from [111] with permission.

2D hybrid perovskites have been repeatedly reported to exhibit strong exciton-phonon coupling. Thus, γ_{ac} and γ_{LO} in 2D $PEAPbI_4$ (phenylethylammonium lead iodide) were found more than ten times higher than that in inorganic quantum wells [112]. Electron phonon-coupling was shown to be highly related to the rate of free exciton (or free charge) trapping, affecting PLQY dramatically. For instance, exciton-phonon coupling in buthylammonium lead iodide was evaluated to be twice as strong as that in phenylethylammonium lead iodide, so the first exhibits a faster nonradiative decay time and lower PLQY [113].

Strong exciton-phonon coupling was shown for phenylethylammonium lead iodide by optical absorbance and photoluminescence spectroscopy at 15 K. At such a low temperature excitonic peaks split to a few peaks, separated by 40–43 meV due to exciton-phonon coupling [114]. Coupling to coherent phonons in the organic cations was observed for the same material by means of transient absorption spectroscopy [115].

When exciton-phonon interaction strength exceeds some critical value, excitons get immobilized, creating is the so-called self-trapped excitons (polarons) and often occurs in polar semiconductors [83]. Self-trapped excitons is an intrinsic phenomenon. If the material also contains defects or impurities, excitons may bound to the defects, forming (extrinsic) trapped excitons. Moreover, excitons may be self-trapped near the defects, causing bounding energy that differs from the intrinsic self-trapping. These three scenarios are schematically shown in Fig. 6 and are described with examples below.

Excitons in many 2D perovskites tend to bound to defects and impurities; radiative and nonradiative pathways taking place depending on the type of the defect (Fig. 7). Different types of defects always take place, caused by chemical impurities, vacancies, or faults. If the defect does not fit the parent lattice well enough, it induces a cloud of distorted host structure around the defect. Excitons can be trapped by this distorted structure, causing typical extrinsic luminescence. These excitons are called trapped or bound excitons. The energy of the photon, emitted from the bound exciton state, is always lower than that of the free exciton one. The difference is equal to the binding energy between the exciton and the impurity. The value depends on the chemical nature of the defect, donor–acceptor behavior and charge [116,117] (p 80;180).

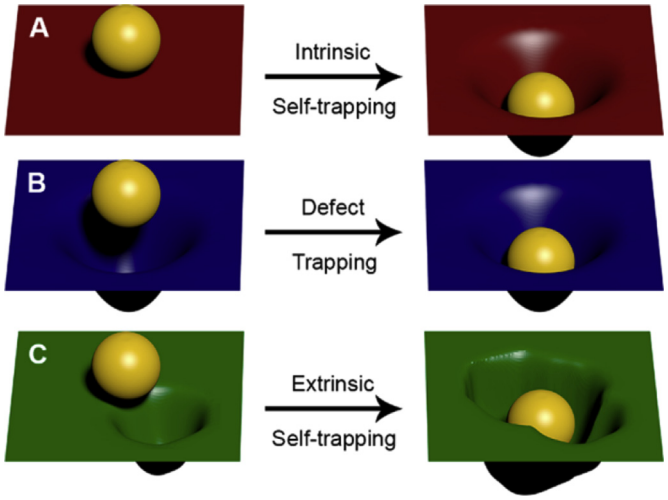

Fig. 6. A) Self-trapped exciton; B) exciton, trapped by a defect; C) extrinsic self-trapping, affected by defects. The ball represents exciton, the surface is potential energy. Adapted with permission from reference [122]. Copyright (2018) American Chemical Society.

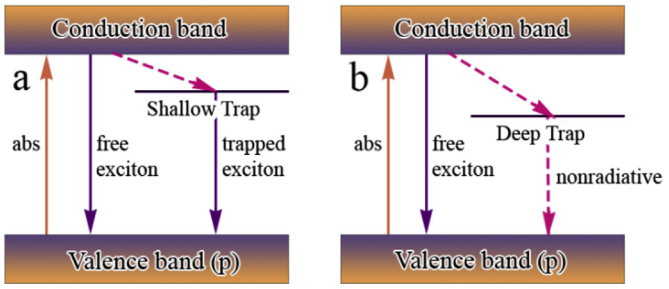

Fig. 7. Schemes of the radiative (a) and nonradiative (b) trapping of electrons (or excitons). Dash line represents nonradiative recombination pathways, the solid one correspond to radiative recombination.

Some 2D perovskites were shown to exhibit emission from trapped excitonic energy levels due to defects. Both shallow and deep trapped excitons were found in $(C_{10}H_{21}NH_3)_2PbI_4$ [70]. The binding energy of the shallow trapped excitons is not very high and normally it yields radiative recombination from the trapper level. The ratio of free and bound excitons increases with the increase of temperature, due to thermal energy activation [70]. The same explanation of the additional red-shifted peak, more intense at low temperature, was provided for $(PEA)_2PbI_4$ [112,114], $(BA)_2(MA)_{n-1}PbnI_{3n+1}$ [41], $(BA)_2PbnI_4$ (shallow, neutral donor trapped excitons) [27], $(PEA)_2(MA)_{n-1}PbnI_{3n+1}$ (shallow defects) [118]. The formation of iodine-related shallow defects was proposed in low-dimensional perovskites in contrast with MA^+-related defects in 3D perovskites. Moreover, large organic cations are able to suppress defects and hysteresis, which is useful for solar cell applications [118].

Deep trapping usually leads to nonradiative decay. The existence of exciton trapping was shown by Gauthron et al. based on temperature-dependent PL intensity in phenyl ethyl ammonium lead iodide. The obtained value of activation energy was far from reported exciton binding energy, besides being sample dependent, and was attributed to nonradiative defects-traps [112].

Another evidence of the trapped states was provided through power-dependent emission intensity. PL intensity grows in a power law function, $I_{PL} \sim I_{ex}^{k}$, where k is the power law coefficient, reflecting the recombination mechanism. In case of free exciton recombination $k = 1$, while presence of the trapped states yields $k = 1.5$, exhibiting saturation behavior at high excitation intensities [119,120].

Self-trapping of excitons leads to $k = 1$ and it does not exhibit saturation at high excitation intensities, because self-trapping is not limited by concentration of defects [121]. Self-trapping causes temporal lattice deformation disappearing after exciton recombination. Self-trapping is schematically presented in Fig. 6 b [122]. Scheme of electronic levels in case of self-trapping is presented in Fig. 8. Luminescence from the self-trapped exciton (STE) states is normally broad and significantly red shifted from the free exciton peak. The decreased energy of the STE state and shape of the ground state (GS) contribute to the red shift, that together with the increased PL width leads to the realization of white light emission [122].

Some 2D perovskites have been reported to be white light emitters due to self-trapped excitons [54,56,76,121,123,124]. Most of the perovskites exhibiting self-trapping form <110>-oriented perovskite sheets. They are 2 × 2 and $(EDBE)PbBr_4$ [56] (EDBE = 2,2-(ethylenedioxy)- bis(ethylammonium)), 2 × 2 $(N\text{-}MEDA)PbBr_4$ ((N-MEDA = N^1-methylethane-1,2-diammonium) [123], 3 × 3 α- $(DMEN)PbBr_4$ (DMEN = 2-(dimethylamino)ethylamine) [54]. A few examples of <100> white light emitting perovskites are known too: $(EDBE)PbCl_4$ [56], $(C_6H_{11}NH_3)_2PbBr_4$ [124], and (*cis*-CyBMA)$PbBr_3$ (*cis*-CyBMA = Cyclohexane-bis(methylammonium)) [76]. In all cases, the broad-band emission was explained by self-trapped excitons.

Besides the coupling to phonons and defects, two excitons can interact with each other due to the columbic forces, forming so-called biexciton. Relatively high binding energies was shown for 2D perovskites (~40–70 meV for $n = 1$ and ~30 meV for $n = 2$) [43,125]. Biexcitonic photoluminescence exhibits the quadratic dependence of Pl intensity on excitation power [43,125]. Triexcitons were observed in 2D perovskites at high excitation powers as well (10^{12}-10^{14} photons/cm^2). Bilogarithmic power dependence was reported to have a slope of 2.6 [126].

Although exciton binding energies in 2D perovskites are normally very high and the excitons hardly dissociate at room temperature, a special mechanism of the exciton dissociation has been reported for thin films of higher ($n > 2$) members of Ruddlesden-Popper perovskites. Blancon et al. demonstrated that excitons $(BA)_2(MA)_{n-1}PbnI_{3n+1}$ perovskites ($n = 3$–5), dissociate to long-live free carriers at the boundary edges, not losing the energy via nonradiative process and being able to contribute to photocurrent [29].

Besides the above listed excitonic effects, a few rarer phenomena have been observed in particular 2D perovskites. Specifically, Rashba band splitting (splitting of bands with different spins) has been demonstrated in noncentrosymmetric ($C2/m$) $PEA_2MAPb_2I_7$. Although the DFT calculations, giving this space group, are very sensitive and cannot prove the effect, photoluminescence lifetime of the $n = 2$ perovskite is much lower than that of centrosymmetric $n = 1$ or $n = 3$ perovskites, indicating slow indirect thermally activated recombination from the split levels [74]. Two more 2D perovskites have been observed to crystallize in non-centrosymmetric space groups: $(PhMe\text{-}NH_3)_2PbCl_4$ ($Cmc2_1$) [12,127] and $(CH_3NH_3)_2Pb(SCN)_2I_2$ ($Pmn2_1$) [128], being potential materials exhibiting the effect. Rashba or spin splitting makes the 2D perovskites candidates for new applications, such as in spintronic device.

Another interesting physical phenomenon observed in 2D perovskites is optical Stark effect, that is splitting of spectral lines in an external electric field. Spin-selective optical Stark effect has been demonstrated in thin films by means of transient optical absorption spectroscopy. The phenomena can be potentially applied in quantum information [79].

7. Phases at low temperatures

The electronic and optical properties, discussed above, are highly correlative with the crystal structures of the two-dimensional perovskites. Applying high pressure or low temperature to the material is a direct way to affect its crystal structure and to observe the evolution of related physical properties. It may allow us to tune the structure in order to understand what leads to the improved properties and acts a guide for the design of new functionalities. Besides, searching structurally stable materials, that do not undergo any phase transitions, is important for practical applications under extreme conditions, for instance in space applications.

From this point of view, it is important to understand how the incorporation of the long organic cation affects compressibility and stability of the structure under changing temperature and pressure, and how this depends on nature of the cation and thickness of the inorganic layers (n).

Alkylammonium 2D perovskites were shown to crystallize in different phases below room temperature. For example $(C_{10}H_{21}NH_3)_2PbI_4$, one of the most studied 2D lead perovskites undergoes a structural phase transition at ~270K [71]. The other members of $(C_mH_{2m+1}NH_3)_2PbI_4$ family also exhibit phase transitions, except for $m = 6$ [49,70,129]. The transition temperatures

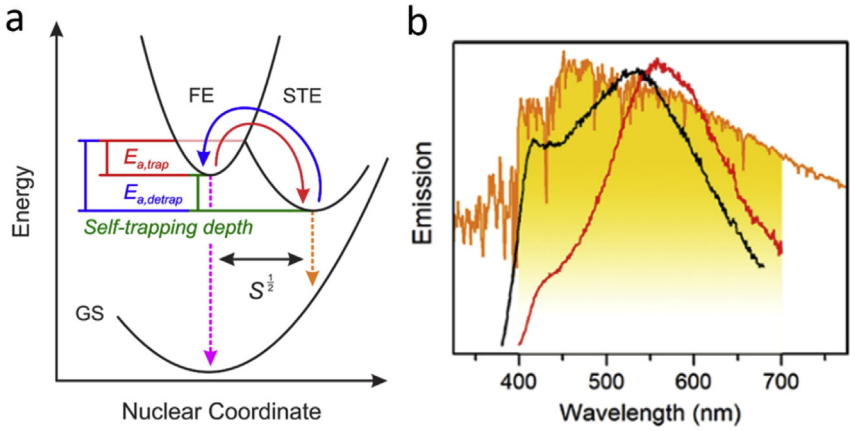

Figure 8. a) Scheme of energy levels in case of self-trapped excitons. Emission (dash lines) occurs from free excitonic state (FE) and self-trapped excitonic state (STE). Red and blue lines represent self-trapping process with activation energy $E_{a,trap}$ and that of detrapping $E_{a,detrap}$. b) White light emission due to self-trapping from (N-MEDA)$PbBr_4$ (red) and (N-MEDA)$PbBr_{3.5}Cl_{0.5}$ (black); the orange line is the Sun spectrum. Adapted with permission from reference [122]. Copyright (2018) American Chemical Society.

correlate the melting temperature of the corresponding amines [32,130](p.308). Unusual optical behavior and phase transitions were reported for $(C_6H_{11}NH_3)_2PbI_4$ (derivative of cyclohexamine), resulting in appearing additional PL peaks at low temperature [131].

In contrast to the alkylammonium perovskites, materials containing benzene ring have not been found to undergo phase transitions at low temperature. For instance, $(PEA)_2SnI_4$ stays in the room temperature phase at least above 125 K [132]. Low-temperature properties of $(PEA)_2PbI_4$ have been reported several times, and no phase transition was found in the range from 10 K to 340 K. However, an inconsistency of the reported data should be emphasized. Thus Son-Tung Ha et al. [82] reported a continuous blue shift of the excitonic PL peak with cooling, while K. Gauthron et al. [112] and T. Ishihara [32] stated a red shift.

$(PEA)_2(MA)Pb_2I_7$ ($n = 2$) was reported to undergo a continuous blue shift excitonic and band edge energies while increasing temperature [94,133], but no detailed information and spectra were shown. Being an intermediate step between 2D and 3D perovskites, these unique materials require a more detailed analysis including their low-temperature behavior.

As for the 3D $MAPbX_3$ perovskites (X = I, Br, Cl), they have been widely studied at various temperatures recently from the optical, structural, and vibrational points of view [15,134,135]. In the range from 80 K to room temperature, the compounds were shown to undergo one to three structural phase transitions (depending on the halogen atoms) from orthorhombic to tetragonal phases followed by a transition to a cubic (only for Cl and I) phase [136]. The transitions are associated with the ordered and disordered state of the MA cation. In case of $MAPbBr_3$, MA cation is fully disordered in the cubic phase, while in the tetragonal hydrogen bonding between NH_3^+ and Br^- freezes the rotation of MA (although the CH_3 end is free), resulting in lowering of symmetry and more distinct Raman MA modes. After the second phase transition, the rearrangement of hydrogen bonding takes place, making the MA totally ordered [135,137,138]. Besides, the stability of the perovskites was reported to be related to hydrogen bonding [139].

According to current finding, the importance of hydrogen bonding in hybrid organic-inorganic perovskites should be considered. Experimental study of hydrogen bonding is a challenging target, because the main structural methods, such as XRD, do not always allow to find exact coordination of the light atoms such as hydrogen. On the other hand, Raman spectroscopy is sensitive to the formation of hydrogen bonds. Raman spectroscopy is a powerful tool to observe the structural changes, especially those involving organic cations.

8. High pressure response

Due to very little high pressure works on 2D perovskites, discussing the high-pressure response of layered perovskites, it is necessary to discuss briefly the parent 3D hybrid perovskite structures.

$MAPbBr_3$ undergoes two phase transitions at very low pressure (<2 GPa) and reversible gradual amorphization at 2–5 GPa [140]. $FAPbBr_3$ is shown to be less compressible, undergoing two phase transitions at higher pressure and amorphization, starting above 4.1 GPa [141]. $MAPbI_3$ undergoes two structural changes as well: 0.3 and 2.5 GPa, followed by gradual amorphization above 2.5 GPa [142,143]. A pressure of 1 GPa that can be reached by chemical methods, is emphasized to be enough to improve the performance in solar cell application [102].

All the described pressure-induced changes are fully reversible (with some hysteresis) for these materials, but some other effects stay permanent after decompression. A phase transition at 0.7 GPa followed by amorphization at 3 GPa was found in $MASnI_3$. Although no amorphization was observed during the second compression process up to 30 GPa. Thus, structural stability was increased by high-pressure applying. Besides, the electrical conductivity and photocurrent of the pressure-treated sample were improved as well [144].

Two competing processes take place under compression: *M-X* bond contraction, and tilting of the octahedra leading to change in the *M-X-M* angle (*M* is, for instance, Pb, *X* is halogen). It is interesting to note that all these materials first exhibit red shift in the band gap under compression that was explained by shrinkage of MX_6 octahedra and contraction of *M-X* bond in cubic or tetragonal phase resulting in stronger *M-X* interaction and hence decrease in the band gap. The tilting of the octahedra, exerting a stronger effect, leads to blue shift of the band gap in lower symmetry phases [141].

There have not been many publications on high-pressure study of layered perovskites by now. However, this is clear that high-pressure response of the layered perovskites is different from the phenomena described above for 3D perovskites. The compression of several members of 2D perovskites does not yield amorphization state in the range up to 30 GPa [34] or leads to it at higher pressure in comparison with 3D perovskites; besides, the first structural changes normally occur under stronger compression too. For example, the first structural changes of octylammonium lead iodide happen at 12 GPa [33], and that of 2D copper (II)–chloride perovskite occurs at 4 GPa [34]. Besides,

although both 3D and 2D perovskites first exhibit a red shift under compression, 3D perovskites then undergo a blue shift, but 2D perovskites do not [33,145].

Thus, two-dimensional perovskites are less compressible and structurally more stable. The effect of different organic cation has not been studied in detail, and the high-pressure response of multi-dimensional perovskites ($n \geq 2$) is a point of interest due to their intermediate nature between 3D and 2D hybrid perovskites. Explanation of the gradual amorphization process in 3D perovskites was proposed to be related to methyl ammonium dynamics and hydrogen bonding [142] that is to be confirmed.

9. Concluding remarks and future outlooks

2D perovskites have been repeatedly shown to be excellent candidates for application in optical devices. The unique properties and outstanding stability allow them to be used in solar cells, LED, spintronics, lasing, and so on. A clear understanding of the fundamental properties is critical for new 2D-perovskite based technologies. In this work, a review of the synthetic methods, physical, structural, and optical properties under various conditions is presented.

Different structural motifs have been discussed. The nature of organic cation has been demonstrated to significantly affect the crystal structure of the 2D perovskites. Thus, the research gaps regarding 2D perovskites are finding new organic molecules to form novel 2D structures, and a deeper understanding of how the organic molecules and their states affects the materials under consideration.

Layered perovskites exhibit special properties, different of these of 3D perovskites. First of all, the natural quantum well structure gives stable excitons with high bonding energies, determining the optical properties even at room temperature. The excitons strongly interact with phonons, sometimes becoming self-trapped, and/or coupled with traps and spins, that makes 2D perovskites very promising materials for novel functionalities and devices. Such phenomena as white light emission, Rashba band splitting, optical Stark effect have been demonstrated in particular members of layered perovskites and are to be studied more completely.

Besides the properties under ambient conditions, the evolution of the properties at low temperature and under high pressure is a point of interest for providing a guide for synthesizing new materials and investigating structural stability. Although the temperature and pressure dependent optical and vibrational properties of 3D hybrid perovskites have been studied in detail, our knowledge of 2D perovskites, especially of multi-dimensional hybrid Huddleston-Popper perovskites, is very limited. These materials act as intermediates between 2D and 3D perovskites that were found to exhibit different behavior under high pressure. Thus, the evolution of the crystal structure and optical properties in these compounds under compression is of special interests.

Finally, improving crystallinity and vertical orientation in order to decrease charge recombination at grain boundaries and by other traps remain an important research topic since this plays a significant role in the device performance.

Competing interests

The authors declare no competing interests.

Acknowledgements

The authors gratefully acknowledge Ministry of Education of Singapore for the funding of this research through the follow grants, AcRF Tier 1 (Reference No: RG103/16); AcRF Tier 1 (RG195/17); AcRF Tier 3 (MOE2016-T3-1-006 (S)).

References

[1] H.F. Kay, P.C. Bailey, Structure and properties of $CaTiO_3$, Acta Crystallogr. 10 (1957) 219, https://doi.org/10.1107/S0365110X57000675.
[2] A. Ferrando, J.P. Martínez Pastor, I. Suárez, Toward metal halide perovskite nonlinear photonics, J. Phys. Chem. Lett. 9 (2018) 5612–5623, https://doi.org/10.1021/acs.jpclett.8b01967.
[3] K.P. Marshall, M. Walker, R.I. Walton, R.A. Hatton, Enhanced stability and efficiency in hole-transport-layer-free $CsSnI_3$ perovskite photovoltaics, Nat. Energy. 1 (2016) 16178, https://doi.org/10.1038/nenergy.2016.178.
[4] E. Dagotto, T. Hotta, A. Moreo, Colossal magnetoresistant materials : the key role of phase separation, Book 344 (2001) 1–153.
[5] L.W. Martin, R. Ramesh, Multiferroic and magnetoelectric heterostructures, Acta Mater. 60 (2012) 2449–2470, https://doi.org/10.1021/acs.jproteome.5b00500.
[6] Q. Chen, N. De Marco, Y. Yang, T. Bin Song, C.C. Chen, H. Zhao, Z. Hong, H. Zhou, Y. Yang, Under the spotlight: the organic-inorganic hybrid halide perovskite for optoelectronic applications, Nano Today 10 (2015) 355–396, https://doi.org/10.1016/j.nantod.2015.04.009.
[7] M.M. Lee, J. Teuscher, T. Miyasaka, T.N. Murakami, H.J. Snaith, Efficient hybrid solar cells based on meso-superstructured organometal halide perovskites, Science 80 (338) (2012) 643–647, https://doi.org/10.1126/science.1228604.
[8] A. Sadhanala, S. Ahmad, B. Zhao, N. Giesbrecht, P.M. Pearce, F. Deschler, R.L.Z. Hoye, K.C. Gödel, T. Bein, P. Docampo, S.E. Dutton, M.F.L. De Volder, R.H. Friend, Blue-Green color tunable solution processable organolead chloride-bromide mixed halide perovskites for optoelectronic applications, Nano Lett. 15 (2015) 6095–6101, https://doi.org/10.1021/acs.nanolett.5b02369.
[9] M.L. Lai, T.Y.S. Tay, A. Sadhanala, S.E. Dutton, G. Li, R.H. Friend, Z.K. Tan, Tunable near-infrared luminescence in tin halide perovskite devices, J. Phys. Chem. Lett. 7 (2016) 2653–2658, https://doi.org/10.1021/acs.jpclett.6b01047.
[10] M.D. Birowosuto, D. Cortecchia, W. Drozdowski, K. Brylew, W. Lachmanski, A. Bruno, C. Soci, X-ray scintillation in lead halide perovskite crystals, Sci. Rep. 6 (2016) 37254, https://doi.org/10.1038/srep37254.
[11] S. Yakunin, M. Sytnyk, D. Kriegner, S. Shrestha, M. Richter, G.J. Matt, H. Azimi, C.J. Brabec, J. Stangl, M.V. Kovalenko, W. Heiss, Detection of X-ray photons by solution-processed lead halide perovskites, Nat. Photon. 9 (2015) 444–449, https://doi.org/10.1038/nphoton.2015.82.
[12] L. Pedesseau, D. Sapori, B. Traore, R. Robles, H.H. Fang, M.A. Loi, H. Tsai, W. Nie, J.C. Blancon, A. Neukirch, S. Tretiak, A.D. Mohite, C. Katan, J. Even, M. Kepenekian, Advances and promises of layered halide hybrid perovskite semiconductors, ACS Nano 10 (2016) 9776–9786, https://doi.org/10.1021/acsnano.6b05944.
[13] D. Ramirez, Y. Suto, N.C. Rosero-Navarro, A. Miura, K. Tadanaga, F. Jaramillo, Structural and electrochemical evaluation of three- and two-dimensional organohalide perovskites and their influence on the reversibility of lithium intercalation, Inorg. Chem. 57 (2018) 4181–4188, https://doi.org/10.1021/acs.inorgchem.8b00397.
[14] G. Xing, N. Mathews, S.S. Lim, N. Yantara, X. Liu, D. Sabba, M. Grätzel, S. Mhaisalkar, T.C. Sum, Low-temperature solution-processed wavelength-tunable perovskites for lasing, Nat. Mater. 13 (2014) 476–480, https://doi.org/10.1038/nmat3911.
[15] R.G. Niemann, A.G. Kontos, D. Palles, E.I. Kamitsos, A. Kaltzoglou, F. Brivio, P. Falaras, P.J. Cameron, Halogen effects on ordering and bonding of $CH_3NH_3^+$ in $CH_3NH_3PbX_3$(X = Cl, Br, I) hybrid perovskites: a vibrational spectroscopic study, J. Phys. Chem. C 120 (2016) 2509–2519, https://doi.org/10.1021/acs.jpcc.5b11256.
[16] J. Yan, W. Qiu, G. Wu, P. Heremans, H. Chen, Recent progress in 2D/quasi-2D layered metal halide perovskites for solar cells, J. Mater. Chem. A. 6 (2018) 11063–11077, https://doi.org/10.1039/c8ta02288g.
[17] C.C. Stoumpos, C.M.M. Soe, H. Tsai, W. Nie, J.C. Blancon, D.H. Cao, F. Liu, B. Traoré, C. Katan, J. Even, A.D. Mohite, M.G. Kanatzidis, High members of the 2D ruddlesden-popper halide perovskites: synthesis, optical properties, and solar cells of $(CH_3(CH_2)_3NH_3)_2(CH_3NH_3)_4Pb_5I_{16}$, Chem 2 (2017) 427–440, https://doi.org/10.1016/j.chempr.2017.02.004.
[18] X. Gan, O. Wang, K. Liu, X. Du, L. Guo, H. Liu, 2D homologous organic-inorganic hybrids as light-absorbers for planer and nanorod-based perovskite solar cells, Sol. Energy Mater. Sol. Cells 162 (2017) 93–102, https://doi.org/10.1016/j.solmat.2016.12.047.
[19] Y. Wei, P. Audebert, L. Galmiche, J.S. Lauret, E. Deleporte, Photostability of 2D organic-inorganic hybrid perovskites, Materials (Basel) 7 (2014) 4789–4802, https://doi.org/10.3390/ma7064789.

[20] N. Wang, L. Cheng, R. Ge, S. Zhang, Y. Miao, W. Zou, C. Yi, Y. Sun, Y. Cao, R. Yang, Y. Wei, Q. Guo, Y. Ke, M. Yu, Y. Jin, Y. Liu, Q. Ding, D. Di, L. Yang, G. Xing, H. Tian, C. Jin, F. Gao, R.H. Friend, J. Wang, W. Huang, Perovskite light-emitting diodes based on solution-processed self-organized multiple quantum wells, Nat. Photon. 10 (2016) 699–704, https://doi.org/10.1038/nphoton.2016.185.

[21] M. Yuan, L.N. Quan, R. Comin, G. Walters, R. Sabatini, O. Voznyy, S. Hoogland, Y. Zhao, E.M. Beauregard, P. Kanjanaboos, Z. Lu, D.H. Kim, E.H. Sargent, Perovskite energy funnels for efficient light-emitting diodes, Nat. Nanotechnol. 11 (2016) 872–877, https://doi.org/10.1038/nnano.2016.110.

[22] D. Li, P. Liao, X. Shai, W. Huang, S. Liu, H. Li, Y. Shen, M. Wang, Recent progress on stability issues of organic-inorganic hybrid lead perovskite-based solar cells, RSC Adv. 6 (2016) 89356–89366, https://doi.org/10.1039/c6ra19801e.

[23] D.H. Cao, C.C. Stoumpos, O.K. Farha, J.T. Hupp, M.G. Kanatzidis, 2D homologous perovskites as light-absorbing materials for solar cell applications, J. Am. Chem. Soc. 137 (2015) 7843–7850, https://doi.org/10.1021/jacs.5b03796.

[24] D.B. Mitzi, C.A. Feild, W.T.A. Harrison, A.M. Guloy, Conducting tin halides with a layered organic-based perovskite structure, Nature 369 (1994) 467–469, https://doi.org/10.1038/369467a0.

[25] D.B. Mitzi, Templating and structural engineering in organic-inorganic perovskites, J. Chem. Soc., Dalton Trans. (2001) 1–12, https://doi.org/10.1039/b007070j.

[26] L.N. Quan, M. Yuan, R. Comin, O. Voznyy, E.M. Beauregard, S. Hoogland, A. Buin, A.R. Kirmani, K. Zhao, A. Amassian, D.H. Kim, E.H. Sargent, Ligand-Stabilized reduced-dimensionality perovskites, J. Am. Chem. Soc. 138 (2016) 2649–2655, https://doi.org/10.1021/jacs.5b11740.

[27] M.H. Jung, Photovoltaic effect of 2D homologous perovskites, Electrochim. Acta 240 (2017) 98–107, https://doi.org/10.1016/j.electacta.2017.04.067.

[28] H. Tsai, W. Nie, J.C. Blancon, C.C. Stoumpos, R. Asadpour, B. Harutyunyan, A.J. Neukirch, R. Verduzco, J.J. Crochet, S. Tretiak, L. Pedesseau, J. Even, M.A. Alam, G. Gupta, J. Lou, P.M. Ajayan, M.J. Bedzyk, M.G. Kanatzidis, A.D. Mohite, High-efficiency two-dimensional ruddlesden-popper perovskite solar cells, Nature 536 (2016) 312–317, https://doi.org/10.1038/nature18306.

[29] J.C. Blancon, H. Tsai, W. Nie, C.C. Stoumpos, L. Pedesseau, C. Katan, M. Kepenekian, C.M.M. Soe, K. Appavoo, M.Y. Sfeir, S. Tretiak, P.M. Ajayan, M.G. Kanatzidis, J. Even, J.J. Crochet, A.D. Mohite, Extremely efficient internal exciton dissociation through edge states in layered 2D perovskites, Science 80 (355) (2017) 1288–1292, https://doi.org/10.1126/science.aal4211.

[30] C. Ma, D. Shen, T.W. Ng, M.F. Lo, C.S. Lee, 2D perovskites with short interlayer distance for high-performance solar cell application, Adv. Mater. 30 (2018) 2–7, https://doi.org/10.1002/adma.201800710.

[31] Z. Wang, Q. Lin, F.P. Chmiel, N. Sakai, L.M. Herz, H.J. Snaith, Efficient ambient-air-stable solar cells with 2D-3D heterostructured butylammonium-caesium-formamidinium lead halide perovskites, Nat. Energy. 2 (2017) 17135, https://doi.org/10.1038/nenergy.2017.135.

[32] T. Ishihara, Optical properties of Pb-based inorganic-organic PerovskiteS, in: T. Ogawa, Y. Kanemitsu (Eds.), Opt. Prop. Low-Dimensional Mater., World Scientific, Singapore, 1995, pp. 289–339.

[33] K. Matsuishi, T. Suzuki, S. Onari, E. Gregoryanz, R.J. Hemley, M. H K, Excitonic states of alkylammonium lead-iodide layered perovskite semiconductors under hydrostatic pressure to 25 gpa, Phys. Status Solidi Basic Res. 223 (2001) 177–182, https://doi.org/10.1002/1521-3951(200101)223:1<177::AID-PSSB177>3.0.CO;2-J.

[34] A. Jaffe, Y. Lin, W.L. Mao, H.I. Karunadasa, Pressure-induced conductivity and yellow-to-black piezochromism in a layered Cu-Cl hybrid perovskite, J. Am. Chem. Soc. 137 (2015) 1673–1678, https://doi.org/10.1021/ja512396m.

[35] M.D. Smith, E.J. Crace, A. Jaffe, H.I. Karunadasa, The diversity of layered halide perovskites, Annu. Rev. Mater. Res. 48 (2018) 111–136, https://doi.org/10.1146/annurev-matsci-070317-124406.

[36] J. Jagielski, S. Kumar, W.Y. Yu, C.J. Shih, Layer-controlled two-dimensional perovskites: synthesis and optoelectronics, J. Mater. Chem. C. 5 (2017) 5610–5627, https://doi.org/10.1039/c7tc00538e.

[37] R.K. Misra, B. El Cohen, L. Iagher, L. Etgar, Low-dimensional organic–inorganic halide perovskite: structure, properties, and applications, ChemSusChem 10 (2017) 3712–3721, https://doi.org/10.1002/cssc.201701026.

[38] C. Lan, Z. Zhou, R. Wei, J.C. Ho, Two-dimensional perovskite materials: from synthesis to energy-related applications, Mater, Today Energy 11 (2019) 61–82, https://doi.org/10.1016/j.mtener.2018.10.008.

[39] W. Travis, E.N.K. Glover, H. Bronstein, D.O. Scanlon, R.G. Palgrave, On the application of the tolerance factor to inorganic and hybrid halide perovskites: a revised system, Chem. Sci. 7 (2016) 4548–4556, https://doi.org/10.1039/c5sc04845a.

[40] Z. Cheng, J. Lin, Layered organic-inorganic hybrid perovskites: structure, optical properties, film preparation, patterning and templating engineering, CrystEngComm 12 (2010) 2646–2662, https://doi.org/10.1039/c001929a.

[41] C.C. Stoumpos, D.H. Cao, D.J. Clark, J. Young, J.M. Rondinelli, J.I. Jang, J.T. Hupp, M.G. Kanatzidis, Ruddlesden-Popper hybrid lead iodide perovskite 2D homologous semiconductors, Chem. Mater. 28 (2016) 2852–2867, https://doi.org/10.1021/acs.chemmater.6b00847.

[42] M.E. Kamminga, H.H. Fang, M.R. Filip, F. Giustino, J. Baas, G.R. Blake, M.A. Loi, T.T.M. Palstra, Confinement effects in low-dimensional lead iodide perovskite hybrids, Chem. Mater. 28 (2016) 4554–4562, https://doi.org/10.1021/acs.chemmater.6b00809.

[43] B. Saparov, D.B. Mitzi, Organic-inorganic perovskites: structural versatility for functional materials design, Chem. Rev. 116 (2016) 4558–4596, https://doi.org/10.1021/acs.chemrev.5b00715.

[44] L. Dou, A.B. Wong, Y. Yu, M. Lai, N. Kornienko, S.W. Eaton, A. Fu, C.G. Bischak, J. Ma, T. Ding, N.S. Ginsberg, L.W. Wang, A.P. Alivisatos, P. Yang, Atomically thin two-dimensional Organic-inorganic hybrid perovskites, Science 349 (2015) 1518–1521, https://doi.org/10.1126/science.aac7660.

[45] J. Calabrese, N.L. Jones, R.L. Harlow, N. Herron, D.L. Thorn, Y. Wang, Preparation and characterization of layered lead halide compounds, J. Am. Chem. Soc. 113 (1991) 2328–2330, https://doi.org/10.1021/ja00006a076.

[46] D.B. Mitzi, Synthesis, crystal structure, and optical and thermal properties of (C 4H9NH3)2MI4 (M = Ge, Sn, Pb), Chem. Mater. 8 (1996) 791–800, https://doi.org/10.1021/cm9505097.

[47] R.-Z. Yin, C.H. Yo, Structural and optical properties of the $(C_nH_{2n+1}NH_3)SnCl_4$ (n = 2, 4, 6, 8, and 10) system, Bull. Korean Chem. Soc. 19 (1998) 947–951.

[48] E. Deleporte, Room-Temperature Optical Tunability and Inhomogeneous Broadening in 2D-Layered Organic – Inorganic Perovskite Pseudobinary Alloys, 2014, https://doi.org/10.1021/jz502086e.

[49] H. Abid, A. Trigui, A. Mlayah, E.K. Hlil, Y. Abid, Phase transition in organic-inorganic perovskite $(C_9H_{19}NH_3)_2PbI_2Br_2$of long-chain alkylammonium, Results Phys 2 (2012) 71–76, https://doi.org/10.1016/j.rinp.2012.04.003.

[50] D. Mitzi, A layered solution crystal growth technique and the crystal structure of $(C_6H_5C_2H_4NH_3)_2PbCl_4$, J. Solid State Chem. 145 (1999) 694–704, https://doi.org/10.1006/jssc.1999.8281.

[51] M. Braun, W. Tuffentsammer, H. Wachtel, H.C. Wolf, Tailoring of energy levels in lead chloride based layered perovskites and energy transfer between the organic and inorganic planes, Chem. Phys. Lett. 303 (1999) 157–164, https://doi.org/10.1016/S0009-2614(99)00205-5.

[52] L. Mao, H. Tsai, W. Nie, L. Ma, J. Im, C.C. Stoumpos, C.D. Malliakas, F. Hao, M.R. Wasielewski, A.D. Mohite, M.G. Kanatzidis, Role of organic counterion in lead- and tin-based two-dimensional semiconducting iodide perovskites and application in planar solar cells, Chem. Mater. 28 (2016) 7781–7792, https://doi.org/10.1021/acs.chemmater.6b03054.

[53] C.A. Chess, A.M. Guloy, C.A. Feild, D.B. Mitzi, S. Wang, Conducting layered organic-inorganic halides containing <110>-Oriented perovskite sheets, Science 80 (267) (2006) 1473–1476, https://doi.org/10.1126/science.267.5203.1473.

[54] L. Mao, Y. Wu, C.C. Stoumpos, M.R. Wasielewski, M.G. Kanatzidis, White-light emission and structural distortion in new corrugated two-dimensional lead bromide perovskites, J. Am. Chem. Soc. 139 (2017) 5210–5215, https://doi.org/10.1021/jacs.7b01312.

[55] J. Yin, H. Li, D. Cortecchia, C. Soci, J.L. Brédas, Excitonic and polaronic properties of 2D hybrid organic-inorganic perovskites, ACS Energy Lett 2 (2017) 417–423, https://doi.org/10.1021/acsenergylett.6b00659.

[56] D. Cortecchia, J. Yin, A. Bruno, S.Z.A. Lo, G.G. Gurzadyan, S. Mhaisalkar, J.L. Brédas, C. Soci, Polaron self-localization in white-light emitting hybrid perovskites, J. Mater. Chem. C. 5 (2017) 2771–2780, https://doi.org/10.1039/c7tc00366h.

[57] T. Dammak, N. Fourati, H. Boughzala, A. Mlayah, Y. Abid, X-ray diffraction, vibrational and photoluminescence studies of the self-organized quantum well crystal $H_3N(CH_2)_6NH_3PbBr_4$, J. Lumin. 127 (2007) 404–408, https://doi.org/10.1016/j.jlumin.2007.01.018.

[58] D.B. Mitzi, K. Chondroudis, C.R. Kagan, Design, structure, and optical properties of Organic–Inorganic perovskites containing an oligothiophene chromophore, Inorg. Chem. 38 (1999) 6246–6256, https://doi.org/10.1021/ic991048k.

[59] S. Shao, J. Liu, G. Portale, H.H. Fang, G.R. Blake, G.H. ten Brink, L.J.A. Koster, M.A. Loi, Highly reproducible Sn-based hybrid perovskite solar cells with 9% efficiency, Adv. Energy Mater. 8 (2018), https://doi.org/10.1002/aenm.201702019.

[60] J.W. Lee, Z. Dai, T.H. Han, C. Choi, S.Y. Chang, S.J. Lee, N. De Marco, H. Zhao, P. Sun, Y. Huang, Y. Yang, 2D perovskite stabilized phase-pure formamidinium perovskite solar cells, Nat. Commun. 9 (2018) 1–10, https://doi.org/10.1038/s41467-018-05454-4.

[61] M. Dion, M. Ganne, M. Tournoux, Nouvelles familles de phases $M^IM^{II}_2Nb_3O_{10}$ a feuillets “perovskites, Mater. Res. Bull. 16 (1981) 1429–1435, https://doi.org/10.1016/0025-5408(81)90063-5.

[62] L. Mao, W. Ke, L. Pedesseau, Y. Wu, C. Katan, J. Even, M.R. Wasielewski, C.C. Stoumpos, M.G. Kanatzidis, Hybrid dion-jacobson 2D lead iodide perovskites, J. Am. Chem. Soc. 140 (2018) 3775–3783, https://doi.org/10.1021/jacs.8b00542.

[63] C.M.M. Soe, C.C. Stoumpos, M. Kepenekian, B. Traoré, H. Tsai, W. Nie, B. Wang, C. Katan, R. Seshadri, A.D. Mohite, J. Even, T.J. Marks, M.G. Kanatzidis, New type of 2D perovskites with alternating cations in the interlayer space, $(C(NH_2)_3)(CH_3NH_3)_nPb_nI3_{n+1}$: structure, properties, and photovoltaic performance, J. Am. Chem. Soc. 139 (2017) 16297–16309, https://doi.org/10.1021/jacs.7b09096.

[64] D.B. Mitzi, Solution-processed inorganic semiconductors, J. Mater. Chem. 14 (2004) 2355–2365, https://doi.org/10.1039/b403482a.

[65] N.R. Venkatesan, J.G. Labram, M.L. Chabinyc, Charge-carrier dynamics and crystalline texture of layered ruddlesden-popper hybrid lead iodide perovskite thin films, ACS Energy Lett 3 (2018) 380–386, https://doi.org/10.1021/acsenergylett.7b01245.

[66] A.Z. Chen, M. Shiu, J.H. Ma, M.R. Alpert, D. Zhang, B.J. Foley, D.M. Smilgies, S.H. Lee, J.J. Choi, Origin of vertical orientation in two-dimensional metal halide perovskites and its effect on photovoltaic performance, Nat. Commun. 9 (2018) 1–7, https://doi.org/10.1038/s41467-018-03757-0.

[67] W. Fu, J. Wang, L. Zuo, K. Gao, F. Liu, D.S. Ginger, A.K.Y. Jen, Two-dimensional perovskite solar cells with 14.1% power conversion efficiency and 0.68% external radiative efficiency, ACS Energy Lett 3 (2018) 2086–2093, https://doi.org/10.1021/acsenergylett.8b01181.

[68] Y. Chen, Y. Sun, J. Peng, W. Zhang, X. Su, K. Zheng, T. Pullerits, Z. Liang, Tailoring organic cation of 2D air-stable organometal halide perovskites for highly efficient planar solar cells, Adv. Energy Mater. 7 (2017) 1–7, https://doi.org/10.1002/aenm.201700162.

[69] T. Ishihara, J. Takahashi, T. Goto, Exciton state in two-dimensional perovskite semiconductor $(C_{10}H_{21}NH_3)_2PbI_4$, Solid State Commun. 69 (1989) 933–936, https://doi.org/10.1016/0038-1098(89)90935-6.

[70] T. Ishihara, J. Takahashi, T. Goto, Optical properties due to electronic transitions in two-dimensional semiconductors $(C_nH_{2n+1}NH_3)_2PbI_4$, Phys. Rev. B 42 (1990) 11099–11107, https://doi.org/10.1103/PhysRevB.42.11099.

[71] T. Ishihara, Optical properties of PbI-based perovskite structures, J. Lumin. 60–61 (1994) 269–274, https://doi.org/10.1016/0022-2313(94)90145-7.

[72] F.O. Saouma, C.C. Stoumpos, J. Wong, M.G. Kanatzidis, J.I. Jang, Selective enhancement of optical nonlinearity in two-dimensional organic-inorganic lead iodide perovskites, Nat. Commun. 8 (2017) 742, https://doi.org/10.1038/s41467-017-00788-x.

[73] C.M.M. Soe, W. Nie, C.C. Stoumpos, H. Tsai, J.C. Blancon, F. Liu, J. Even, T.J. Marks, A.D. Mohite, M.G. Kanatzidis, Understanding film formation morphology and orientation in high member 2D ruddlesden–popper perovskites for high-efficiency solar cells, Adv. Energy Mater 8 (2018) 1–10, https://doi.org/10.1002/aenm.201700979.

[74] J. Yin, P. Maity, L. Xu, A.M. El-Zohry, H. Li, O.M. Bakr, J.-L. Brédas, O.F. Mohammed, Layer-dependent Rashba band splitting in 2D hybrid perovskites, Chem. Mater. 3 (2018), https://doi.org/10.1021/acs.chemmater.8b03436 acs.chemmater.8b03436.

[75] O. Nazarenko, M.R. Kotyrba, S. Yakunin, M. Aebli, G. Rainò, B.M. Benin, M. Wörle, M.V. Kovalenko, Guanidinium-formamidinium lead iodide: a layered perovskite-related compound with red luminescence at room temperature, J. Am. Chem. Soc. 140 (2018) 3850–3853, https://doi.org/10.1021/jacs.8b00194.

[76] I. Neogi, A. Bruno, D. Bahulayan, T.W. Goh, B. Ghosh, R. Ganguly, D. Cortecchia, T.C. Sum, C. Soci, N. Mathews, S.G. Mhaisalkar, Broadband-emitting 2 D hybrid organic–inorganic perovskite based on cyclohexane-bis(methylammonium) cation, ChemSusChem 10 (2017) 3765–3772, https://doi.org/10.1002/cssc.201701227.

[77] K. Tanaka, T. Takahashi, T. Kondo, K. Umeda, K. Ema, T. Umebayashi, K. Asai, K. Uchida, N. Miura, Electronic and excitonic structures of inorganic-organic perovskite-type quantum-well crystal $(C_4H_9NH_3)_2PbBr_4$, Japanese J. Appl. Physics 44 (2005) 5923–5932, https://doi.org/10.1143/JJAP.44.5923. Part 1 Regul. Pap. Short Notes Rev. Pap.

[78] D.H. Cao, C.C. Stoumpos, T. Yokoyama, J.L. Logsdon, T. Bin Song, O.K. Farha, M.R. Wasielewski, J.T. Hupp, M.G. Kanatzidis, Thin films and solar cells based on semiconducting two-dimensional ruddlesden-popper $(CH_3(CH_2)_3NH_3)_2(CH_3NH_3)_n-1Sn_nI_{3n+1}$Perovskites, ACS Energy Lett 2 (2017) 982–990, https://doi.org/10.1021/acsenergylett.7b00202.

[79] D. Giovanni, W.K. Chong, H.A. Dewi, K. Thirumal, I. Neogi, R. Ramesh, S. Mhaisalkar, N. Mathews, T.C. Sum, Tunable room-temperature spin-selective optical Stark effect in solution-processed layered halide perovskites, Sci. Adv. 2 (2016) 1–6, https://doi.org/10.1126/sciadv.1600477.

[80] M. Era, T. Kobayashi, K. Sakaguchi, E. Tsukamoto, Y. Oishi, Electric conduction of PbBr-based layered perovskite organic-inorganic superlattice having carbazole chromophore-linked ammonium molecule as an organic layer, Org. Electron. Physics, Mater. Appl. 14 (2013) 1313–1317, https://doi.org/10.1016/j.orgel.2013.02.008.

[81] X. Yang, X. Zhang, J. Deng, Z. Chu, Q. Jiang, J. Meng, P. Wang, L. Zhang, Z. Yin, J. You, Efficient green light-emitting diodes based on quasi-two-dimensional composition and phase engineered perovskite with surface passivation, Nat. Commun. 9 (2018) 2, https://doi.org/10.1038/s41467-018-02978-7.

[82] S.T. Ha, C. Shen, J. Zhang, Q. Xiong, Laser cooling of organic-inorganic lead halide perovskites, Nat. Photon. 10 (2016) 115–121, https://doi.org/10.1038/nphoton.2015.243.

[83] Z. Guo, X. Wu, T. Zhu, X. Zhu, L. Huang, Electron-phonon scattering in atomically thin 2D perovskites, ACS Nano 10 (2016) 9992–9998, https://doi.org/10.1021/acsnano.6b04265.

[84] O. Yaffe, A. Chernikov, Z.M. Norman, Y. Zhong, A. Velauthapillai, A. Van Der Zande, J.S. Owen, T.F. Heinz, Excitons in ultrathin organic-inorganic perovskite crystals, Phys. Rev. B Condens. Matter 92 (2015) 1–7, https://doi.org/10.1103/PhysRevB.92.045414.

[85] Z. Chen, Y. Wang, X. Sun, Y. Guo, Y. Hu, E. Wertz, X. Wang, H. Gao, T.M. Lu, J. Shi, Van der Waals hybrid perovskite of high optical quality by chemical vapor deposition, Adv. Opt. Mater. 5 (2017) 1–8, https://doi.org/10.1002/adom.201700373.

[86] D. Liang, Y. Peng, Y. Fu, M.J. Shearer, J. Zhang, J. Zhai, Y. Zhang, R.J. Hamers, T.L. Andrew, S. Jin, Color-pure violet-light-emitting diodes based on layered lead halide perovskite nanoplates, ACS Nano 10 (2016) 6897–6904, https://doi.org/10.1021/acsnano.6b02683.

[87] B. El Cohen, M. Wierzbowska, L. Etgar, High efficiency and high open circuit voltage in quasi 2D perovskite based solar cells, Adv. Funct. Mater. 27 (2017) 1604733, https://doi.org/10.1002/adfm.201604733.

[88] T. Zhang, M.I. Dar, G. Li, F. Xu, N. Guo, M. Grätzel, Y. Zhao, Bication lead iodide 2D perovskite component to stabilize inorganic a-CsPbI3perovskite phase for high-efficiency solar cells, Sci. Adv. 3 (2017) 1–7, https://doi.org/10.1126/sciadv.1700841.

[89] X. Li, M. Ibrahim Dar, C. Yi, J. Luo, M. Tschumi, S.M. Zakeeruddin, M.K. Nazeeruddin, H. Han, M. Grätzel, Improved performance and stability of perovskite solar cells by crystal crosslinking with alkylphosphonic acid ω-ammonium chlorides, Nat. Chem. 7 (2015) 703–711, https://doi.org/10.1038/nchem.2324.

[90] G. Grancini, C. Roldán-Carmona, I. Zimmermann, E. Mosconi, X. Lee, D. Martineau, S. Narbey, F. Oswald, F. De Angelis, M. Graetzel, M.K. Nazeeruddin, One-Year stable perovskite solar cells by 2D/3D interface engineering, Nat. Commun. 8 (2017) 15684, https://doi.org/10.1038/ncomms15684.

[91] Y. Takeoka, M. Fukasawa, T. Matsui, K. Kikuchi, M. Rikukawa, K. Sanui, Intercalated formation of two-dimensional and multi-layered perovskites in organic thin films, Chem. Commun. (2005) 378–380, https://doi.org/10.1039/b413398f.

[92] A. Vassilakopoulou, D. Papadatos, I. Zakouras, I. Koutselas, Mixtures of quasi-two and three dimensional hybrid organic-inorganic semiconducting perovskites for single layer LED, J. Alloy. Comp. 692 (2017) 589–598, https://doi.org/10.1016/j.jallcom.2016.09.076.

[93] X. Wu, M.T. Trinh, D. Niesner, H. Zhu, Z. Norman, J.S. Owen, O. Yaffe, B.J. Kudisch, X.Y. Zhu, Trap states in lead iodide perovskites, J. Am. Chem. Soc. 137 (2015) 2089–2096, https://doi.org/10.1021/ja512833n.

[94] X. Hong, T. Ishihara, A.V. Nurmikko, Dielectric confinement effect on excitons in PbI_4-based layered semiconductors, Phys. Rev. B 45 (1992) 6961–6964, https://doi.org/10.1103/PhysRevB.45.6961.

[95] M.D. Smith, L. Pedesseau, M. Kepenekian, I.C. Smith, C. Katan, J. Even, H.I. Karunadasa, Decreasing the electronic confinement in layered perovskites through intercalation, Chem. Sci. 8 (2017) 1960–1968, https://doi.org/10.1039/c6sc02848a.

[96] M. Qasim, M.S. Wismer, M. Agarwal, V.S. Yakovlev, Optical Properties of Laser-Excited Solids, Oxford, 2018, https://doi.org/10.1119/1.1691372.

[97] T. Fujita, H. Nakashima, M. Hirasawa, T. Ishihara, Ultrafast photoluminescence from $(C_6H_5C_2H_4NH_3)_2PbI_4$, J. Lumin. 87 (2000) 847–849, https://doi.org/10.1016/S0022-2313(99)00437-8.

[98] J. Wong, M.G. Kanatzidis, J.I. Jang, Selective enhancement of optical nonlinearity in two-dimensional organic-inorganic lead iodide perovskites, Nat. Commun. (2017) 1–7, https://doi.org/10.1038/s41467-017-00788-x.

[99] J. Even, L. Pedesseau, C. Katan, Understanding quantum confinement of charge carriers in layered 2D hybrid perovskites, ChemPhysChem 15 (2014) 3733–3741, https://doi.org/10.1002/cphc.201402428.

[100] T. Umebayashi, K. Asai, T. Umebayashi, K. Asai, T. Kondo, T. Kondo, A. Nakao, Electronic structures of lead iodide based low-dimensional crystals, Phys. Rev. B Condens. Matter 67 (2003) 155405, https://doi.org/10.1103/PhysRevB.67.155405.

[101] D. Cortecchia, S. Neutzner, A.R.S. Kandada, E. Mosconi, D. Meggiolaro, F. De Angelis, C. Soci, A. Petrozza, Broadband emission in two-dimensional hybrid perovskites: the role of structural deformation, J. Am. Chem. Soc. 139 (2017) 39–42, https://doi.org/10.1021/jacs.6b10390.

[102] A. Jaffe, Y. Lin, C.M. Beavers, J. Voss, W.L. Mao, H.I. Karunadasa, High-pressure single-crystal structures of 3D lead-halide hybrid perovskites and pressure effects on their electronic and optical properties, ACS Cent. Sci. 2 (2016) 201–209, https://doi.org/10.1021/acscentsci.6b00055.

[103] L. Gan, J. Li, Z. Fang, H. He, Z. Ye, Effects of organic cation length on exciton recombination in two-dimensional layered lead iodide hybrid perovskite crystals, J. Phys. Chem. Lett. 8 (2017) 5177–5183, https://doi.org/10.1021/acs.jpclett.7b02083.

[104] K. Chondroudis, D.B. Mitzi, Electroluminescence from an organic-inorganic perovskite incorporating a quaterthiophene dye within lead halide perovskite layers, Chem. Mater. 11 (1999) 3028–3030, https://doi.org/10.1021/cm990561t.

[105] K. Ema, M. Inomata, Y. Kato, H. Kunugita, M. Era, Nearly perfect triplet-triplet energy transfer from wannier excitons to naphthalene in organic-inorganic hybrid quantum-well materials, Phys. Rev. Lett. 100 (2008) 1–4, https://doi.org/10.1103/PhysRevLett.100.257401.

[106] A.E. Maughan, J.A. Kurzman, J.R. Neilson, Hybrid inorganic-organic materials with an optoelectronically active aromatic cation: (C7H7)2SnI6and C7H7PbI3, Inorg. Chem. 54 (2015) 370–378, https://doi.org/10.1021/ic5025795.

[107] J.J. Liu, Y.F. Guan, C. Jiao, M.J. Lin, C.C. Huang, W.X. Dai, A panchromatic hybrid crystal of iodoplumbate nanowires and J-aggregated naphthalene diimides with long-lived charge-separated states, Dalton Trans. 44 (2015) 5957–5960, https://doi.org/10.1039/c4dt03785e.

[108] S. Maheshwari, T.J. Savenije, N. Renaud, F.C. Grozema, Computational design of two-dimensional perovskites with functional organic cations, J. Phys. Chem. C 122 (2018) 17118–17122, https://doi.org/10.1021/acs.jpcc.8b05715.

[109] B. Cheng, T. Li, P. Maity, P. Wei, D. Nordlund, D. Lien, C. Lin, R. Liang, X. Miao, I.A. Ajia, J. Yin, A. Javey, I.S. Roqan, O.F. Mohammed, J. He, K. Ho, Extremely reduced dielectric confinement in two-dimensional hybrid perovskites with

large polar organics, Commun. Phys. (2018), https://doi.org/10.1038/s42005-018-0082-8.
[110] M. Ueta, H. Kanzaki, K. Kobayashi, Y. Toyozawa, E. Hanamura, Excitonic Processes in Solids, Springer Berlin Heidelberg, Berlin, Heidelberg, 1986, https://doi.org/10.1007/978-3-642-82602-3.
[111] A.D. Wright, C. Verdi, R.L. Milot, G.E. Eperon, M.A. Pérez-Osorio, H.J. Snaith, F. Giustino, M.B. Johnston, L.M. Herz, Electron-phonon coupling in hybrid lead halide perovskites, Nat. Commun. 7 (2016), https://doi.org/10.1038/ncomms11755.
[112] K. Gauthron, J. Lauret, L. Doyennette, G. Lanty, A. Al Choueiry, S.J. Zhang, A. Brehier, L. Largeau, O. Mauguin, J. Bloch, E. Deleporte, Optical spectroscopy of two-dimensional layered $(C_6H_5C_2H_4NH_3)_2PbI_4$ perovskite, Optic Express 18 (2010) 5912, https://doi.org/10.1364/OE.18.005912.
[113] X. Gong, O. Voznyy, A. Jain, W. Liu, R. Sabatini, Z. Piontkowski, G. Walters, G. Bappi, S. Nokhrin, O. Bushuyev, M. Yuan, R. Comin, D. McCamant, S.O. Kelley, E.H. Sargent, Electron-phonon interaction in efficient perovskite blue emitters, Nat. Mater. 17 (2018) 550–556, https://doi.org/10.1038/s41563-018-0081-x.
[114] D.B. Straus, S. Hurtado Parra, N. Iotov, J. Gebhardt, A.M. Rappe, J.E. Subotnik, J.M. Kikkawa, C.R. Kagan, Direct observation of electron-phonon coupling and slow vibrational relaxation in organic-inorganic hybrid perovskites, J. Am. Chem. Soc. 138 (2016) 13798–13801, https://doi.org/10.1021/jacs.6b08175.
[115] D. Giovanni, W.K. Chong, Y.Y.F. Liu, H.A. Dewi, T. Yin, Y. Lekina, Z.X. Shen, N. Mathews, C.K. Gan, T.C. Sum, Coherent spin and quasiparticle dynamics in solution-processed layered 2D lead halide perovskites, Adv. Sci. 1800664 (2018), https://doi.org/10.1002/advs.201800664.
[116] N.U. Yasuo Nakayama, Steffen Duhm, Xin Qian, Satoshi Kera, Hisao Ishii, Electronic Processes in Organic Crystals, Second ed., Oxford University Press, New York, 2015 https://doi.org/10.1007/978-4-431-55206-2.
[117] I. Pelant, J. Valenta, Luminescence of excitons, in: Lumin. Spectrosc. Semicond., 2012, pp. 161–204, https://doi.org/10.1093/acprof:oso/9780199588336.003.0007.
[118] W. Peng, J. Yin, K.T. Ho, O. Ouellette, M. De Bastiani, B. Murali, O. El Tall, C. Shen, X. Miao, J. Pan, E. Alarousu, J.H. He, B.S. Ooi, O.F. Mohammed, E. Sargent, O.M. Bakr, Ultralow self-doping in two-dimensional hybrid perovskite single crystals, Nano Lett. 17 (2017) 4759–4767, https://doi.org/10.1021/acs.nanolett.7b01475.
[119] T. Schmidt, K. Lischka, W. Zulehner, Excitation-power dependence of the near-band-edge photoluminescence of semiconductors, Phys. Rev. B 45 (1992) 8989–8994, https://doi.org/10.1103/PhysRevB.45.8989.
[120] S. Draguta, S. Thakur, Y.V. Morozov, Y. Wang, J.S. Manser, P.V. Kamat, M. Kuno, Spatially non-uniform trap state densities in solution-processed hybrid perovskite thin films, J. Phys. Chem. Lett. 7 (2016) 715–721, https://doi.org/10.1021/acs.jpclett.5b02888.
[121] M.D. Smith, A. Jaffe, E.R. Dohner, A.M. Lindenberg, H.I. Karunadasa, Structural origins of broadband emission from layered Pb-Br hybrid perovskites, Chem. Sci. 8 (2017) 4497–4504, https://doi.org/10.1039/c7sc01590a.
[122] M.D. Smith, H.I. Karunadasa, White-light emission from layered halide perovskites, Acc. Chem. Res. 51 (2018) 619–627, https://doi.org/10.1021/acs.accounts.7b00433.
[123] T. Hu, M.D. Smith, E.R. Dohner, M.J. Sher, X. Wu, M.T. Trinh, A. Fisher, J. Corbett, X.Y. Zhu, H.I. Karunadasa, A.M. Lindenberg, Mechanism for broadband white-light emission from two-dimensional (110) hybrid perovskites, J. Phys. Chem. Lett. 7 (2016) 2258–2263, https://doi.org/10.1021/acs.jpclett.6b00793.
[124] S. Pillet, D. Garrot, A. Yangui, M. Castro, S. Triki, K. Boukheddaden, Y. Abid, G. Bouchez, E.E. Bendeif, J.S. Lauret, A. Lusson, E. Deleporte, Optical investigation of broadband white-light emission in self-assembled organic–inorganic perovskite $(C_6H_{11}NH_3)_2PbBr_4$, J. Phys. Chem. C 119 (2015) 23638–23647, https://doi.org/10.1021/acs.jpcc.5b06211.
[125] D. Giovanni, T.W. Goh, T.C. Sum, X. Liu, W.K. Chong, K. Thirumal, N. Mathews, S. Mhaisalkar, Dominant factors limiting the optical gain in layered two-dimensional halide perovskite thin films, Phys. Chem. Chem. Phys. 18 (2016) 14701–14708, https://doi.org/10.1039/c6cp01955b.
[126] S. Capponi, D. Poilblanc, Photoluminescence of the inorganic-organic layered semiconductor $(C_6H_5C_2H_4NH_3)_2PbI_4$: observation of triexciton formation, Phys. Rev. B 75 (2007) 092406, https://doi.org/10.1103/PhysRevB.75.092406.
[127] W.Q. Liao, Y. Zhang, C.L. Hu, J.G. Mao, H.Y. Ye, P.F. Li, S.D. Huang, R.G. Xiong, A lead-halide perovskite molecular ferroelectric semiconductor, Nat. Commun. 6 (2015) 7338, https://doi.org/10.1038/ncomms8338.
[128] M. Daub, H. Hillebrecht, Synthesis, single-crystal structure and characterization of $(CH_3NH_3)_2Pb(SCN)_2I_2$, Angew. Chem. Int. Ed. 54 (2015) 11016–11017, https://doi.org/10.1002/anie.201506449.
[129] Y. Abid, X-ray and Raman studies of the re-entrant phase and phase transitions in the perovskite-type layer compound bis(n-propylammonium) lead tetrabromide, J. Phys. Condens. Matter 6 (1994) 6447–6454, https://doi.org/10.1088/0953-8984/6/32/007.
[130] E.A. Muljarov, S.G. Tikhodeev, N.A. Gippius, T. Ishihara, Excitons in self-organized semiconductor/insulator superlattices: PbI-based perovskite compounds, Phys. Rev. B 51 (1995) 14370–14378, https://doi.org/10.1103/PhysRevB.51.14370.
[131] A. Yangui, S. Pillet, A. Mlayah, A. Lusson, G. Bouchez, S. Triki, Y. Abid, K. Boukheddaden, Structural phase transition causing anomalous photoluminescence behavior in perovskite $(C_6H_{11}NH_3)_2[PbI_4]$, J. Chem. Phys. 143 (2015), https://doi.org/10.1063/1.4936776.
[132] G.C. Papavassiliou, I.B. Koutselas, A. Terzis, M.H. Whangbo, Structural and electronic properties of the natural quantum-well system $(C_6H_5CH_2CH_2NH_3)_2SnI_4$, Solid State Commun. 91 (1994) 695–698, https://doi.org/10.1016/0038-1098(94)00435-8.
[133] T. Kataoka, T. Kondo, R. Ito, S. Sasaki, K. Uchida, N. Miura, Magneto-optical effects of excitons in the layered perovskite-type material $(C_6H_{13}NH_3)_2(CH_3NH_3)Pb2I7$, Phys. B Phys. Condens. Matter. 201 (1994) 423–426, https://doi.org/10.1016/0921-4526(94)91129-0.
[134] M.I. Dar, G. Jacopin, S. Meloni, A. Mattoni, N. Arora, A. Boziki, S.M. Zakeeruddin, U. Rothlisberger, M. Grätzel, Origin of unusual bandgap shift and dual emission in organic-inorganic lead halide perovskites, Sci. Adv. 2 (2016), https://doi.org/10.1126/sciadv.1601156 e1601156–e1601156.
[135] T. Yin, Y. Fang, X. Fan, B. Zhang, J.-L. Kuo, T.J. White, G.M. Chow, J. Yan, Z.X. Shen, Hydrogen-bonding evolution during the polymorphic transformations in $CH_3NH_3PbBr_3$: experiment and theory, Chem. Mater. 29 (2017) 5974–5981, https://doi.org/10.1021/acs.chemmater.7b01630.
[136] A.M.A. Leguy, A.R. Goñi, J.M. Frost, J. Skelton, F. Brivio, X. Rodríguez-Martínez, O.J. Weber, A. Pallipurath, M.I. Alonso, M. Campoy-Quiles, M.T. Weller, J. Nelson, A. Walsh, P.R.F. Barnes, Dynamic disorder, phonon lifetimes, and the assignment of modes to the vibrational spectra of methylammonium lead halide perovskites, Phys. Chem. Chem. Phys. 18 (2016) 27051–27066, https://doi.org/10.1039/c6cp03474h.
[137] J.H. Lee, J.H. Lee, E.H. Kong, H.M. Jang, The nature of hydrogen-bonding interaction in the prototypic hybrid halide perovskite, tetragonal $CH_3NH_3PbI_3$, Sci. Rep. 6 (2016) 1–12, https://doi.org/10.1038/srep21687.
[138] J.H. Lee, N.C. Bristowe, P.D. Bristowe, A.K. Cheetham, Role of hydrogen-bonding and its interplay with octahedral tilting in $CH_3NH_3PbI_3$, Chem. Commun. 51 (2015) 6434–6437, https://doi.org/10.1039/c5cc00979k.
[139] F. El-Mellouhi, A. Marzouk, E.T. Bentria, S.N. Rashkeev, S. Kais, F.H. Alharbi, Hydrogen bonding and stability of hybrid organic–inorganic perovskites, ChemSusChem 9 (2016) 2648–2655, https://doi.org/10.1002/cssc.201600864.
[140] Y. Wang, X. Lü, W. Yang, T. Wen, L. Yang, X. Ren, L. Wang, Z. Lin, Y. Zhao, Pressure-induced phase transformation, reversible amorphization, and anomalous visible light response in organolead bromide perovskite, J. Am. Chem. Soc. 137 (2015) 11144–11149, https://doi.org/10.1021/jacs.5b06346.
[141] L. Wang, K. Wang, B. Zou, Pressure-induced structural and optical properties of organometal halide perovskite-based formamidinium lead bromide, J. Phys. Chem. Lett. 7 (2016) 2556–2562, https://doi.org/10.1021/acs.jpclett.6b00999.
[142] M. Szafrański, A. Katrusiak, Mechanism of pressure-induced phase transitions, amorphization, and absorption-edge shift in photovoltaic methylammonium lead iodide, J. Phys. Chem. Lett. 7 (2016) 3458–3466, https://doi.org/10.1021/acs.jpclett.6b01648.
[143] T. Ou, J. Yan, C. Xiao, W. Shen, C. Liu, X. Liu, Y. Han, Y. Ma, C. Gao, Visible light response, electrical transport, and amorphization in compressed organolead iodine perovskites, Nanoscale 8 (2016) 11426–11431, https://doi.org/10.1039/c5nr07842c.
[144] X. Lü, Y. Wang, C.C. Stoumpos, Q. Hu, X. Guo, H. Chen, L. Yang, J.S. Smith, W. Yang, Y. Zhao, H. Xu, M.G. Kanatzidis, Q. Jia, Enhanced structural stability and photo responsiveness of $CH_3NH_3SnI_3$Perovskite via pressure-induced amorphization and recrystallization, Adv. Mater. 28 (2016) 8663–8668, https://doi.org/10.1002/adma.201600771.
[145] K. Matsuishi, T. Ishihara, S. Onari, Y.H. Chang, C.H. Park, Optical properties and structural phase transitions of lead-halide based inorganic-organic 3D and 2D perovskite semiconductors under high pressure, Phys. Status Solidi Basic Res. 241 (2004) 3328–3333, https://doi.org/10.1002/pssb.200405229.